

# Accelerating Longitudinal MRI using Prior Informed Latent Diffusion

Yonatan Urman<sup>\*,1</sup>, Zachary Shah<sup>\*,1</sup>, Ashwin Kumar<sup>2</sup>, Bruno P.Soaes<sup>2</sup>, and Kawin Setsompop<sup>1,2</sup>

<sup>1</sup> Department of Electrical Engineering, Stanford University

<sup>2</sup> Department of Radiology, Stanford University

**Abstract.** MRI is a widely used ionization-free soft-tissue imaging modality, often employed repeatedly over a patient’s lifetime. However, prolonged scanning durations, among other issues, can limit availability and accessibility. In this work, we aim to substantially reduce scan times by leveraging prior scans of the same patient. These prior scans typically contain considerable shared information with the current scan, thereby enabling higher acceleration rates when appropriately utilized. We propose a prior informed reconstruction method with a trained diffusion model in conjunction with data-consistency steps. Our method can be trained with unlabeled image data, eliminating the need for a dataset of either k-space measurements or paired longitudinal scans as is required of other learning-based methods. We demonstrate superiority of our method over previously suggested approaches in effectively utilizing prior information without over-biasing prior consistency, which we validate on both an open-source dataset of healthy patients as well as several longitudinal cases of clinical interest.

**Keywords:** MRI Reconstruction · Longitudinal MRI · Latent Diffusion.

## 1 Introduction

Magnetic Resonance Imaging (MRI) remains a prevalent medical procedure, often repeated throughout a patient’s life [20,30,28,29]. However, it faces challenges such as lengthy scan times and motion-related artifacts compromising image quality. Consequently, limited accessibility to MRI and extended waiting times are common [2]. This is detrimental for certain patient populations, such as children, who may find extended scanning times challenging and may require sedation, which can have long-term effects [9]. Accelerating the MRI scanning process is therefore desirable, improving patient throughput and accessibility.

The fundamental MRI reconstruction problem can be formulated as follows:

$$\hat{\mathbf{x}} = \arg \min_{\mathbf{x}} \|\mathcal{A}(\mathbf{x}) - \mathbf{y}\|_2^2 + \lambda \mathcal{R}(\mathbf{x}) \quad (1)$$

---

\* Equal contribution

Here,  $\mathcal{A}$ ,  $\mathbf{x}$ , and  $\mathbf{y}$  denote the MRI forward operator, the image intended for reconstruction, and the k-space measurements, respectively.  $\mathcal{R}(\mathbf{x})$  is a regularizer which typically incorporates prior knowledge [11,16]. Recently, deep learning-based models have gained popularity due to their capacity to efficiently represent complex priors and integrate into an iterative reconstruction scheme [1]. Notably, diffusion models have been proposed to act as deep priors [24,10,19,4,13,15], where the inference process of a trained model is guided by data consistency (DC) steps to enforce alignment with the acquired measurements. Since training a generative model only necessitates access to reconstructed images, this approach can leverage vast existing datasets of MR images, eliminating the need for acquiring pairs of k-space and reconstructed images as would be required for other supervised learning methods. Moreover, confining the use of measurements to inference alone permits utilization of one trained model with various measurement operators, such as different trajectories or subsampling schemes.

While the concepts presented in this study are applicable broadly, our primary focus specifically examines brain MRI. In clinical settings, patients frequently undergo multiple scans to monitor the progression of some neurological condition. These conditions often manifest as subtle and localized changes in the morphology and contrast of brain matter. Surprisingly, information from prior MRI scans is rarely utilized during the formation of subsequent scans, despite perceptual similarity in the reconstructed images. One potential explanation for this lies in the difficulty of accurately quantifying the relationship between prior scan ( $\mathbf{x}^{\text{prior}}$ ) and subsequent scan ( $\mathbf{x}^{\text{new}}$ ), as forming the conditional distribution  $p(\mathbf{x}^{\text{new}}|\mathbf{x}^{\text{prior}})$  requires modeling numerous factors such as aging, disease state, and more. Even if successfully modeled, properly utilizing this relationship in reconstruction remains unclear. As a proxy for  $p(\mathbf{x}^{\text{new}}|\mathbf{x}^{\text{prior}})$ , previous works add  $\lambda_2 f(\mathbf{x}^{\text{new}}, \mathbf{x}^{\text{prior}})$  as an additional regularization term to (1) in order to capture scan similarities in the image domain [27]. However, this approach is highly sensitive to both image registration and hyper-parameters, especially the regularization parameter  $\lambda_2$ . Over-scaling  $\lambda_2$  can lead to a reconstruction too similar to the prior, neglecting crucial differences. Conversely, under-setting  $\lambda_2$  could result in disregarding the prior, thereby missing potential acceleration.

Recently, score-based models [25] have achieved leading capability in modeling high-dimensional distributions. Rather than modeling  $p(\mathbf{x}^{\text{new}}|\mathbf{x}^{\text{prior}})$ , we assume  $\mathbf{x}^{\text{prior}}$  and  $\mathbf{x}^{\text{new}}$  are drawn from the same distribution  $p(\mathbf{x})$ , which we represent with a score-based latent diffusion model (LDM), subsequently guiding the reconstruction process within the manifold of such a distribution. In implementation, we employ a state-of-the-art pre-trained LDM, namely Stable Diffusion (SD) [21], improving training time, output image fidelity, and generalization compared to training from scratch. We hypothesize that integrating prior information into this deep latent representation will facilitate higher subsampling rates, enabling to shorter scan times.

The main contributions of our work are: **(i)** We introduce a novel longitudinal reconstruction framework based on LDMs, which demonstrates superior performance compared to previous approaches. **(ii)** We demonstrate that such

a latent-based framework decreases the sensitivity of reconstruction to prior image alignment, eliminating the the need for prior-scan registration. **(iii)** Our proposed approach can be trained without k-space measurements or a paired dataset of sequential scans, both of which are challenging to acquire and impede training for other supervised learning-based longitudinal reconstruction schemes. **(iv)** We showcase SD in a medical imaging setting, offering an efficient gateway for pre-trained foundational models for such applications.

## 2 Background

### 2.1 Score-based Models

Score-based models [25,8] operate on the principle of gradually transforming samples from an initial distribution  $p_0(\mathbf{x})$  to samples from an unstructured noise distribution such as  $\mathcal{N}(0, \mathbf{I})$  using a forward stochastic differential equation (SDE). This process can be reversed to sample from  $p_0(\mathbf{x})$  given the score function  $\nabla_{\mathbf{x}} \log p(\mathbf{x})$ . In the commonly employed variance preserving case from [25] the reverse SDE is given by:

$$d\mathbf{x} = \left[-\frac{\beta_t}{2}\mathbf{x} - \beta_t \nabla_{\mathbf{x}} \log p(\mathbf{x})\right] dt + \sqrt{\beta_t} d\mathbf{w} \quad (2)$$

Here,  $\beta_t$  is a noise scheduling parameter that monotonically increases with  $t \in [0, T]$ , and  $\mathbf{w}$  is a Wiener process. Initiating  $\mathbf{x}_T \sim \mathcal{N}(0, \mathbf{I})$  and following this reverse SDE from  $t = T$  to  $t = 0$  results in  $\mathbf{x}_0 \sim p(\mathbf{x})$ . Since the true score function is generally unknown, score-based models parameterize it using a neural network optimized via denoising score matching, represented as  $\mathbf{s}_\theta(\mathbf{x}, t)$  [26].

To better condition the learning of the score function, LDMs perform the denoising process in a latent space, compressing important image features into a lower-dimensional distribution. This is achieved by first training an autoencoder with encoder  $\mathcal{E}$  and decoder  $\mathcal{D}$ , then training the diffusion process to model  $\mathbf{z}_0 = \mathcal{E}(\mathbf{x}_0)$ . LDMs exhibit computational efficiency by conducting all operations within this reduced-dimensional space while achieving exceptional image quality.

Stable Diffusion comprises a family of models that conditionally guide the image generation process using text. These models were trained on billions of natural images, enabling them to serve as robust pre-trained models. By fine-tuning SD with a new dataset, such as brain MRI images, SD can tailor its foundational knowledge of high-quality generation towards a specific application.

### 2.2 Solving Inverse Problems with Score-based Models

Inverse problems such as (1) involve reconstructing a signal  $\mathbf{x}$  given noisy measurements  $\mathbf{y}$ , typically in an ill-posed setting, necessitating the assumption that  $\mathbf{x}$  is sampled from some prior distribution  $p(\mathbf{x})$ . An efficient reconstruction algorithm in this scenario is posterior sampling [3,22,23], which involves sampling from the distribution  $p(\mathbf{x}|\mathbf{y})$ . This can be effectively implemented using

score-based models by modifying Equation (2) at some timestep  $t$  to utilize the conditional score function  $\nabla_{\mathbf{x}_t} \log p(\mathbf{x}_t|\mathbf{y}) = \nabla_{\mathbf{x}_t} \log p(\mathbf{y}|\mathbf{x}_t) + \nabla_{\mathbf{x}_t} \log p(\mathbf{x}_t)$ . Thus, a learned prior  $p(\mathbf{x})$  can guide sampling using DC steps corresponding to  $\nabla_{\mathbf{x}_t} \log p(\mathbf{y}|\mathbf{x}_t)$  [10,3]. Solving inverse problems with LDMs presents an interesting challenge due to the diffusion process occurring in the latent space, meaning we must now instead compute  $\nabla_{\mathbf{z}_t} \log p(\mathbf{y}|\mathbf{z}_t)$  for DC. To tackle this, [23] proposed hard DC with resampling, where during some predefined steps of the diffusion process, the current diffusion step  $\mathbf{z}_t$  is projected back as  $\hat{\mathbf{z}}_0 = \mathbb{E}[\mathbf{z}_0|\mathbf{z}_t]$  using Tweedie’s formula [5] to initialize solving  $\hat{\mathbf{z}}_0^* = \arg \min_{\mathbf{z}} \|\mathbf{y} - \mathcal{A}(\mathcal{D}(\mathbf{z}))\|_2^2$  using first-order optimization methods. Afterwards,  $\hat{\mathbf{z}}_0^*$  is projected forward to  $t$  using stochastic resampling. Such resampling can diverge from the latent manifold if the data-consistent sample deviates far from  $\mathbb{E}[\mathbf{z}_0|\mathbf{z}_t]$ . As an alternative, the authors of [22] proposed estimating  $\nabla_{\mathbf{z}_t} \log p(\mathbf{y}|\mathbf{z}_t) = \nabla_{\mathbf{z}_t} \log p(\mathbf{y}|\mathcal{D}(\mathbb{E}[\mathbf{z}_0|\mathbf{z}_t]))$ . They further suggested enforcing  $\mathbf{z}_t$  to be a fixed point of the autoencoder to better condition gradient optimization. We found this method favorable since it optimizes  $\mathbf{z}_t$  directly, whereas the resampling step of hard DC tended to produce blurrier images in our experiments.

### 3 Method

We consider the longitudinal reconstruction setting with one prior scan  $\mathbf{x}^{\text{prior}}$  and noisy measurements of a new scan  $\mathcal{A}(\mathbf{x})$ . We propose a learning-based approach and assume access to a dataset of scans to learn a prior distribution, subsequently utilized for reconstruction through DC-augmented latent diffusive posterior sampling. For DC, we employ a method akin to the one proposed in [22]. Specifically, on every diffusion step, we execute several Adam [12] optimization steps to minimize  $\|\mathbf{y} - \mathcal{A}(\mathcal{D}(\mathbb{E}[\mathbf{z}_0|\mathbf{z}_t]))\|_2^2$  over  $\mathbf{z}_t$  to align the diffusion sample with the measurements, where,  $\mathbb{E}[\mathbf{z}_0|\mathbf{z}_t] = (\mathbf{z}_t + \sqrt{1 - \bar{\alpha}_t} \mathbf{s}_\theta(\mathbf{z}_t, t)) / \sqrt{\bar{\alpha}_t}$ .

We take advantage of the fact that all scans *originate from the same distribution*, a valid assumption when using a sufficiently diverse training dataset. Therefore, instead of randomly sampling noise as the initial image for posterior reconstruction and relying solely on DC steps to steer the diffusion process towards generating the acquired image, we propose initializing the reverse process *using the prior scan*. Specifically, we select a timestep  $t^p \in (0, T)$ , where the signal-to-noise ratio is low enough to permit the diffusion process to generate images notably different from the prior, yet not too low so that it can utilize information from the prior for reconstruction. This way, we ”hot start” the diffusion process with latent features from the prior scan, and let the DC-augmented sampling guide it to the new scan. We term this method Prior Informed Posterior Sampling (PIPS) and summarize it in Algorithm 1.

Our choice of employing LDMs for reconstruction is motivated by the fact that MR images can be effectively represented in a lower-dimensional space [16,7,18]. Training a high-quality image generation model with an LDM generally requires massive datasets and countless GPU hours to accurately fit some distribution. Instead, we opt to fine-tune SD which facilitates learning an image

distribution with a knowledge base of image semantics SD would have learned to represent, enabling faster training with a smaller-scale datasets.

Since text conditioning is utilized in SD but is not of primary importance to our task, we used a constant prompt and enabled gradients to flow to its embedding during fine-tuning, similar to Textual Inversion [6]. This strategy allows the model to find an optimal text embedding representation that aids in producing more accurate images from the new dataset.

For our prior conditioning, PIPS employs a softer form of conditioning during inference by using the prior as an initialization in the sampling process. Thus, we aim to learn only an unconditional image generation model, allowing us to train a model without the need for sequential scan pairs. Moreover, PIPS is forward-model agnostic, enabling the same model and method to be employed with different undersampling once the prior has been learned.

---

**Algorithm 1:** PIPS

---

**Input:** Trained latent score function:  $\mathbf{s}_\theta(\mathbf{z}, t)$ , Prior image:  $\mathbf{x}^{\text{prior}}$ , Prior projection timestep:  $t^p$ , Number of optimization steps:  $n_{\text{opt}}$

- 1  $\mathbf{z}^{\text{prior}} = \mathcal{E}(\mathbf{x}^{\text{prior}})$ ; // Compute prior’s latent representation
- 2  $\mathbf{z}_{t^p}^{\text{prior}} = \sqrt{\bar{\alpha}_{t^p}}\mathbf{z}^{\text{prior}} + (1 - \bar{\alpha}_{t^p})\mathbf{n}$   $\mathbf{n} \sim \mathcal{N}(0, 1)$ ; // Project to  $t^p$
- 3 **for**  $t = t^p$  **to** 1 **do**
- 4      $\mathbf{z}_t = \arg \min_{\mathbf{z}_t} \|\mathbf{y} - \mathcal{A}(\mathcal{D}(\mathbb{E}[\mathbf{z}_0|\mathbf{z}_t]))\|_2^2$ ; // DC for  $n_{\text{opt}}$  steps
- 5      $\mathbf{z}_{t-1} = \text{Diffusion}(\mathbf{z}_t, \mathbf{s}_\theta(\mathbf{z}_t, t))$ ; // Reverse diffusion step
- 6 **end**
- 7 **return**  $\mathbf{x} = \mathcal{D}(\mathbf{z}_0)$ ; // Reconstructed image

---

## 4 Evaluation

To evaluate the proposed approach, we utilized two datasets for SD fine-tuning. The first is the open-source OASIS dataset [14], from which we curated 273 patients with longitudinal T1-weighted scans, resulting in a dataset of size 62720 2D slices, holding out 1000 paired slices for testing (note that sequentially paired scans are only required for testing; for training we treat all scans as independent examples). The second dataset was obtained from a local hospital containing 10 longitudinal pairs of T1-weighted scans from different patients, accepted for use by local IRB. We used data from 8 patients for training (3000 slices), withholding 2 pairs of patient scans (100 slices) for testing. To assess performance, we measured the average peak signal-to-noise ratio (pSNR) and structural similarity index (SSIM) over two groupings of patches within an image. To form these groupings, we segmented the ground truth longitudinal data pair into  $32 \times 32$  patches and computed the normalized cross-correlation of each. Patches with correlation above 0.95 were marked similar, otherwise marked as dissimilar. This segmented  $\sim 30\%$  of patches in both datasets as similar. Average pSNR and SSIM were then calculated between the reconstruction and ground truth for these patch groupings. This separation is crucial since metric computation in this setting is challenging (i.e., simply copying the prior can falsely score well). Our

patch-grouped metrics assess both effectiveness in utilizing prior information in relevant areas, while scrutinizing performance in areas susceptible to prior bias.

For our method, we use  $t_p = 200$  as the prior projection timepoint (where the diffusion process was trained with 1000 timepoints) and perform DC optimization at every diffusion step. We compare the proposed method with prior regularized conjugate-gradient reconstruction [17] minimizing  $\|y - \mathcal{A}(\mathbf{x})\|_2 + \lambda\|\mathbf{x}\|_2^2 + \lambda_p\|\mathbf{x} - \mathbf{x}^{\text{prior}}\|_2^2$  (**CG-Prior**), Longitudinal Adaptive Compressed Sensing (**LACS**) [27], our method without the prior (**LDPS**), and **MODL** [1], a learning-based unrolled framework interleaving a learned denoising prior with data fidelity. As a proof of concept, we simulated complex multi-coil k-space measurements with 12 coils and uniformly under-sampled with a 1D Cartesian mask in the anterior-posterior direction, retaining a fully sampled center k-space (5%). Although our code is not currently publicly available due to the double-blind review process, we will release it, including all trained models and implementation details, once the review process is complete.

Table 1 shows the performance of all methods at different acceleration rates  $R$ . For small acceleration rates, where the reconstruction is not so ill posed, PIPS and MODL perform similarly. However, for high  $R$ , our method outperforms the baselines. It is worth noting that our method does not necessitate k-space data for training, unlike MODL, which makes MODL less adaptable to different protocols. Figure 1 demonstrates a reconstruction example from the OASIS test dataset for various acceleration factors. While we see that most methods perform reasonably well on similar patches, ours outperforms the other methods on the patches that are not similar, especially for  $R \geq 6$ .

A limitation of many prior-utilizing reconstruction schemes is the sensitivity to prior alignment. We find that PIPS works well even with mis-registered priors, as exemplified by Figure 2. PIPS succeeds over other image-domain methods like

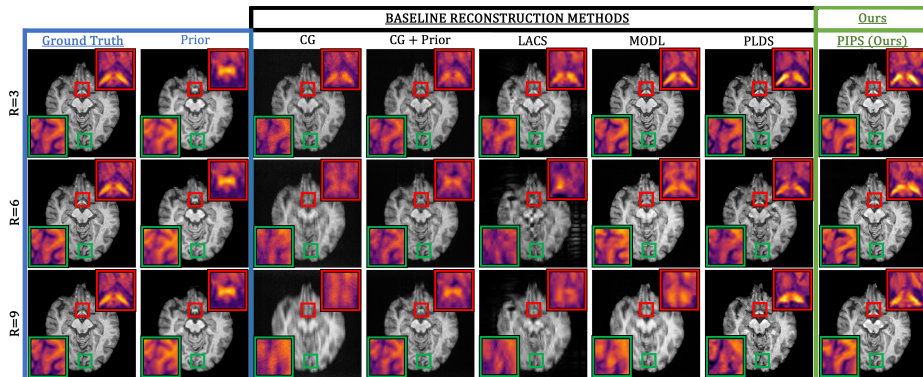


Fig. 1: Reconstructions vs acceleration ( $R$ ). Learning-based (MODL, PLDS) baselines lose quality in prior-similar ROI (green) at  $R = 9$ . Prior-informed (CG+Prior, LACS) methods over-bias towards prior in dis-similar ROI (red) with increased  $R$ . PIPS maintains highest fidelity in both regions.

CG-Prior and LACS, likely because the latent domain introduces some level of rotational and slice invariance (see supplementary for further examples).

Of particular interest in the longitudinal image reconstruction setting is the specificity to features correlated to medical differentials. Training a full-scale foundational model to represent all possible clinical progressions and post-operational changes poses a challenge due to the difficulty in collecting a diverse enough dataset. As a proof-of-concept, we fine-tuned the LDM we trained on OASIS with 3000 image slices from local hospital cases exhibiting the progression of various tumors and lesions. To evaluate generalizability, Figure 3 depicts a reconstruction example for the fine-tuned model on an unseen clinical case before and after placement of an ommaya reservoir through the left frontal cortex. We observe that only PIPS can both detect the catheter and produce a high-

Acceleration	pSNR (similar/dis-similar)   SSIM (similar/dis-similar)				
	Ours (PIPS)	LDPS	MODL	LACS	CG-Prior
3	32.45/33	30/30	<u>33.7/34.5</u>	24.3/26.6	29.1/26.8
	0.88/0.88	0.85/0.87	<u>0.92/0.91</u>	0.69/0.66	0.78/0.7
6	<u>29.4/29.8</u>	26/27	<u>29.5/30.3</u>	22.1/22.8	27/22.7
	0.82/0.81	0.76/0.79	<u>0.85/0.84</u>	0.64/0.52	0.74/0.55
9	<u>25.3/26.2</u>	21.5/24	23/24.1	18.3/18.7	25.4/19.5
	<u>0.73/0.73</u>	0.6/0.7	0.69/0.67	0.52/0.35	0.71/0.42
12	<u>25.2/26.1</u>	18.2/19.3	22.8/23.8	18.7/19	25.5/20
	<u>0.72/0.72</u>	0.46/0.4	0.67/0.65	0.53/0.35	0.71/0.42

Table 1: pSNR and SSIM at different acceleration rates evaluated on our test set of OASIS. The upper (lower) row of each item is the pSNR (SSIM) and the split is (similar/dis-similar patches). Best result in each category is underlined.

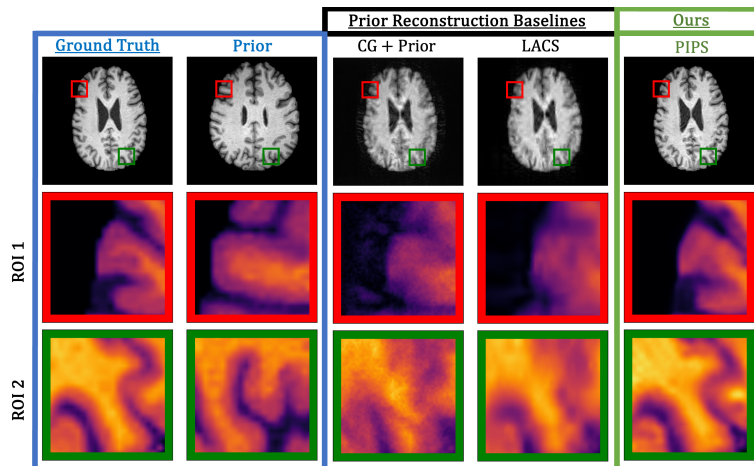


Fig. 2: Reconstruction for unregistered slice in OASIS for R=6. Baselines collapse due to prior dis-similarity; PIPS maintains high quality both locally and overall.

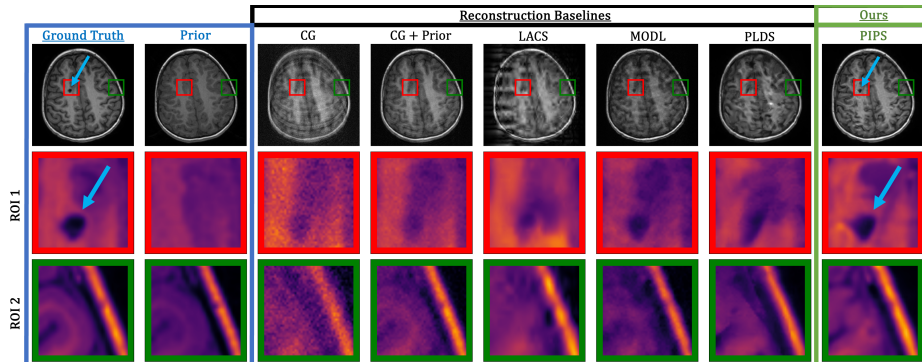


Fig. 3: Catheter placement (ROI 1, blue arrow) for R=6 with registration. Prior-informed baselines (CG+Prior, LACS) only partially construct the catheter due to prior bias. Learning-based baselines (MODL, PLDS) fail to generate sharp image due to high undersampling. PIPS most sharply reconstructs the catheter.

fidelity reconstruction, demonstrating the capability of a learned prior of brain conditions to amplify target features with limited data.

## 5 Summary

We have introduced a simple yet effective method for MRI reconstruction in longitudinal settings. Our proposed approach leverages an LDM, eliminating the need for a supervised dataset for training. Fine-tuning from SD enhances training efficiency and aids in generalization. By initializing the reconstruction with the latent representation of the prior, we enable the model to utilize features of the prior in the reconstruction process. We set the prior projection timepoint to strike a balance between allowing the diffusion process enough flexibility to generate significantly different images while still incorporating information from the prior scan. Operating in latent space helps the model avoid incompatibilities between the prior and the new scan, such as misregistration or slight contrast differences, and enables it to focus on important scan features.

Across all tested acceleration rates, our proposed method outperforms non-learning-based prior approaches. While achieving similar performance to MODL at low acceleration rates, our method outperforms it for higher acceleration rates. Notably, while MODL requires a paired dataset of k-space and reconstructed images, our method does not, allowing training with large open-source image datasets. Furthermore, MODL needs to be retrained for each distinct forward model, whereas our method is forward model agnostic.

An interesting and important avenue for future work would be to explore the incorporation of multiple prior scans, as well as devising a method for averaging during this process. Additionally, finding the optimal projection timepoint  $t_p$  presents an intriguing area of investigation. Utilizing these techniques and mul-



multiple diffusion samples, we can compute an uncertainty map to assist radiologists in determining if additional samples are necessary.

## References

1. Aggarwal, H., Mani, M., Jacob, M.: Modl: Model-based deep learning architecture for inverse problems. *IEEE Transactions on Medical Imaging* **38**(2), 394–405 (Feb 2019). <https://doi.org/10.1109/TMI.2018.2865356>, epub 2018 Aug 13
2. van Beek, E.J., Kuhl, C., Anzai, Y., Desmond, P., Ehman, R.L., Gong, Q., Gold, G., Gulani, V., Hall-Craggs, M., Leiner, T., et al.: Value of mri in medicine: More than just another test? *Journal of Magnetic Resonance Imaging* **49**(7), e14–e25 (2019)
3. Chung, H., Kim, J., Mccann, M.T., Klasky, M.L., Ye, J.C.: Diffusion posterior sampling for general noisy inverse problems. In: *International Conference on Learning Representations (2023)*, <https://openreview.net/forum?id=OnD9zGAGT0k>
4. Dar, S.U., Öztürk, Ş., Korkmaz, Y., Elmas, G., Özbey, M., Güngör, A., Çukur, T.: Adaptive diffusion priors for accelerated mri reconstruction. *arXiv preprint arXiv:2207.05876* (2022)
5. Efron, B.: Tweedie’s formula and selection bias. *Journal of the American Statistical Association* **106**(496), 1602–1614 (2011). <https://doi.org/10.1198/jasa.2011.tm11181>, epub 2012 Jan 24
6. Gal, R., Alaluf, Y., Atzmon, Y., Patashnik, O., Bermano, A.H., Chechik, G., Cohen-Or, D.: An image is worth one word: Personalizing text-to-image generation using textual inversion (2022). <https://doi.org/10.48550/ARXIV.2208.01618>, <https://arxiv.org/abs/2208.01618>
7. Haldar, J.P.: Low-rank modeling of local k-space neighborhoods (loraks) for constrained mri. *IEEE Transactions on Medical Imaging* **33**(3), 668–681 (Mar 2014). <https://doi.org/10.1109/TMI.2013.2293974>
8. Ho, J., Jain, A., Abbeel, P.: Denoising diffusion probabilistic models. *arXiv preprint arxiv:2006.11239* (2020)
9. Ing, C., DiMaggio, C., Whitehouse, A., Hegarty, M.K., Brady, J., von Ungern-Sternberg, B.S., Davidson, A., Wood, A.J., Li, G., Sun, L.S.: Long-term differences in language and cognitive function after childhood exposure to anesthesia. *Pediatrics* **130**(3), e476–e485 (Sep 2012)
10. Jalal, A., Arvinte, M., Daras, G., Price, E., Dimakis, A.G., Tamir, J.I.: Robust compressed sensing mri with deep generative priors. *Advances in Neural Information Processing Systems* (2021)
11. Joshi, S., Marquina, A., Osher, S., Dinov, I., Van Horn, J., Toga, A.: Mri resolution enhancement using total variation regularization. In: *Proceedings of the IEEE International Symposium on Biomedical Imaging*. pp. 161–164 (2009). <https://doi.org/10.1109/ISBI.2009.5193008>
12. Kingma, D., Ba, J.: Adam: A method for stochastic optimization. In: *International Conference on Learning Representations (ICLR)*. San Diego, CA, USA (2015)
13. Korkmaz, Y., Cukur, T., Patel, V.M.: Self-supervised mri reconstruction with unrolled diffusion models. In: Greenspan, H., et al. (eds.) *Medical Image Computing and Computer Assisted Intervention – MICCAI 2023*. *Lecture Notes in Computer Science*, vol. 14229. Springer (2023)
14. LaMontagne, P.J., Benzinger, T.L., Morris, J.C., Keefe, S., Hornbeck, R., Xiong, C., Grant, E., Hassenstab, J., Moulder, K., Vlassenko, A.G., et al.: Oasis-3: longitudinal neuroimaging, clinical, and cognitive dataset for normal aging and alzheimer disease. *MedRxiv* pp. 2019–12 (2019)
15. Luo, G., Blumenthal, M., Heide, F., Uecker, M.: Bayesian mri reconstruction with joint uncertainty estimation using diffusion models. *Magnetic Resonance in Medicine* **90**(1), 295–311 (Jul 2023), epub 2023 Mar 13

16. Lustig, M., Donoho, D., Pauly, J.: Sparse mri: The application of compressed sensing for rapid mr imaging. *Magnetic Resonance in Medicine* **58**(6), 1182–1195 (Dec 2007). <https://doi.org/10.1002/mrm.21391>
17. Maier, O., Baete, S., Fyrdahl, A., Hammernik, K., Harrevelt, S., Kasper, L., Karakuzu, A., Loecher, M., Patzig, F., Tian, Y., Wang, K., Gallichan, D., Uecker, M., Knoll, F.: Cg-sense revisited: Results from the first ismrm reproducibility challenge. *Magnetic Resonance in Medicine* **85**(4), 1821–1839 (Apr 2021). <https://doi.org/10.1002/mrm.28569>
18. Ong, F., Lustig, M.: Beyond low rank + sparse: Multiscale low rank matrix decomposition. *IEEE Journal of Selected Topics in Signal Processing* **10**(4), 672–687 (2016). <https://doi.org/10.1109/JSTSP.2016.2545518>
19. Peng, C., Guo, P., Zhou, S.K., Patel, V.M., Chellappa, R.: Towards performant and reliable undersampled mr reconstruction via diffusion model sampling. In: Wang, L., Dou, Q., Fletcher, P.T., Speidel, S., Li, S. (eds.) *Medical Image Computing and Computer Assisted Intervention – MICCAI 2022*. *Lecture Notes in Computer Science*, vol. 13436. Springer (2022)
20. Rees, J., Watt, H., Jäger, H.R., Benton, C., Tozer, D., Tofts, P., Waldman, A.: Volumes and growth rates of untreated adult low-grade gliomas indicate risk of early malignant transformation. *European Journal of Radiology* **72**(1), 54–64 (Oct 2009). <https://doi.org/10.1016/j.ejrad.2008.06.013>, epub 2008 Jul 15
21. Rombach, R., Blattmann, A., Lorenz, D., Esser, P., Ommer, B.: High-resolution image synthesis with latent diffusion models. In: *Proceedings of the IEEE/CVF Conference on Computer Vision and Pattern Recognition*. pp. 10684–10695 (2022)
22. Rout, L., Raoof, N., Daras, G., Caramanis, C., Dimakis, A.G., Shakkottai, S.: Solving linear inverse problems provably via posterior sampling with latent diffusion models (2023)
23. Song, B., Kwon, S.M., Zhang, Z., Hu, X., Qu, Q., Shen, L.: Solving inverse problems with latent diffusion models via hard data consistency. *arXiv preprint arXiv:2307.08123* (2023)
24. Song, Y., Shen, L., Xing, L., Ermon, S.: Solving inverse problems in medical imaging with score-based generative models. *arXiv preprint arXiv:2111.08005* (2021)
25. Song, Y., Sohl-Dickstein, J., Kingma, D.P., Kumar, A., Ermon, S., Poole, B.: Score-based generative modeling through stochastic differential equations. In: *International Conference on Learning Representations* (2021), <https://openreview.net/forum?id=PxtTIG12RRHS>
26. Vincent, P.: A connection between score matching and denoising autoencoders. *Neural Computation* **23**(7), 1661–1674 (2011)
27. Weizman, L., Eldar, Y., Ben Bashat, D.: Compressed sensing for longitudinal mri: An adaptive-weighted approach. *Medical Physics* **42**(9), 5195–5208 (Sep 2015). <https://doi.org/10.1118/1.4928148>
28. Weizman, L., Sira, L.B., Joskowicz, L., Rubin, D.L., Yeom, K.W., Constantini, S., Shofty, B., Bashat, D.B.: Semiautomatic segmentation and follow-up of multicomponent low-grade tumors in longitudinal brain mri studies. *Medical Physics* **41**(5), 052303 (May 2014). <https://doi.org/10.1118/1.4871040>
29. Young, G.S., Macklin, E.A., Setayesh, K., Lawson, J.D., Wen, P.Y., Norden, A.D., Drappatz, J., Kesari, S.: Longitudinal mri evidence for decreased survival among periventricular glioblastoma. *Journal of Neuro-Oncology* **104**(1), 261–269 (Aug 2011). <https://doi.org/10.1007/s11060-010-0477-1>, epub 2010 Dec 5
30. Zahid, U., Hedges, E.P., Dimitrov, M., Murray, R.M., Barker, G.J., Kempton, M.J.: Impact of physiological factors on longitudinal structural mri measures of the brain. *Psychiatry Research: Neuroimaging* **321**, 111446 (2022)